Advanced Self Climbing Hydraulic Formwork System

Ahmad Samadi , Engineering Building & Infrastructure, contact@ebni.com.au
Dep. of Civil and Environmental Engineering,
Western Sydney University, Sydney, NSW, 2762, 12/07/2025.

Abstract

Currently, self-climbing formworks are frequently employed in the construction of tall concrete structures, including high-rise skyscrapers, silos, and bridge piers. A conventional formwork can be enhanced to incorporate additional functionalities, such as the ability to ascend to the designated building location. The climbing qualities of the formwork, along with the opening and closing features of the formwork shell, are critical parameters for assessing the performance of self-climbing formwork. In contrast to prior research, this paper offers a number of enhancements for certain groups to improve a hydraulic self-climbing formwork's qualities. A new rail clamping mechanism and a new method for opening and closing the formwork shells are proposed based on the composition analysis and operation of the actual climbing formwork types. For the purpose of designing a self-climbing formwork, they are utilised, and the shell's working size is four meters by three meters.
The concrete surface's flatness following casting, as well as its load capacity, are evaluated. The suggested fixes may lead to a number of benefits, such as a quicker initial alignment time, higher-quality concrete surfaces, and the highest level of automation for building processes.

The shortcomings of conventional first-order linear design methods in formwork design standards can be effectively addressed by employing a direct analysis method to design the formwork structure, which is required due to the complex connection of components and significant initial defects in the formwork structure. A direct analysis method for the construction of a SCP structure was proposed, using a practical engineering project as an example. A comparative analysis was conducted with the traditional first-order linear design method to elucidate the impact of initial defects and second-order effects on the support reaction force, deformation, and stress ratio, based on the design results. Structures for SCPs were designed using this as a guide. On the basis of the findings, cross-sectional optimisation was implemented on the primary components of the SCP structure.
The direct analysis method was demonstrated to be feasible in the design and optimisation of the SCP structure, as the stress ratio distribution of the structure was found to be more reasonable following optimisation. Additionally, a 25.63% reduction in steel consumption was achieved.

Introduction

The technology of self-climbing formwork has been extensively utilised in the construction of cast-in-place reinforced concrete structures of considerable height on a global scale. This groundbreaking construction technology proves to be exceptionally advantageous for edifices wherein the walls and floors are constructed autonomously, including silos, bridge piers, lift pits, and the walls of towering skyscrapers(Nguyen et al. 2019). An exemplary instance of the efficacy of employing climbing formwork in the context of high-rise construction is evidenced by the implementation of Doka's systems.

The self-climbing formworks utilised in the construction of the Burj Khalifa Tower, located in Dubai, United Arab Emirates, represent a significant advancement in engineering and architectural methodology. Moreover, in conjunction with the act of pouring concrete into vertical structures, the formwork possesses the capability toUsed to construct buildings with a maximum typical angle of 25 degrees.

According to (Peurifoy & Oberlender 2011), formwork is a temporary structure used to shape and size freshly mixed concrete.

In addition to the live load itself, formwork needs to be large enough to hold the weight of the materials, machinery, and workers generated by new concrete construction.

Engineers and builders are interested in the lateral pressure of fresh concrete because an overestimation of this value raises the cost of formwork,(Hurd 2007) demonstrated can account for up to 60% of the cost of a concrete structure. (Kopczynski 2008) confirms this finding.

An underestimate of the pressure, on the other hand, results in subpar components or, in the worst situation, the structure failing.

According to (Hurd 2007), safety, quality, and cost should be the main goals when designing forms and support elements. As a result, it is essential to understand the lateral pressure of fresh concrete.

In a great number of technical articles, the significance of the topic has been expressed. The most popular method for casting a wall or column is to pour concrete into lifts and then vibrate them. To ensure proper consolidation, the vibrators are immersed in the concrete for a length equivalent to the lift's height. utilising the form wall. Following full fluidisation, the concrete behaves like a fluid, resulting in lateral pressure that is equivalent to the hydrostatic pressure generated by a fluid of the same density as concrete.

Not all of the concrete mass is fluidised, according to (Gardner 1985), since deeper layers are not impacted by vibration and hence gain shear strength, enabling them to sustain vertical loads, create friction between the concrete and the wall, and thereby produce less lateral pressure.

The demand for a variety of automated formwork systems in the construction of high-rise buildings is increasing due to their high efficiency, standardisation, lightweight, and other attributes. This trend is consistent with the accelerated development of these structures. A self-climbing forming and working platform (SCP) is a type of hydraulic lifting formwork that is incorporated for the construction of core-tube structures(Mohan Sai & Aravindan 2020). It can considerably accelerate the construction speed of high-rise structures due to its high load-bearing capacity, high space utilisation rate, and high personnel comfort (Ye et al. 2024).

Shell climbing formwork

At some point above the form's base, the lateral pressure reaches its maximum and then begins to decrease. The formation of chemical compounds at the lower layers results in the development of shear strength and friction with the form wall. According to (Gardner & Poon 1976) , temperature and time are the primary determinants of this process.

Over time, two primary approaches to problem solving have emerged: either create a conceptual model of the issue utilising the mechanical and rheological characteristics of new concrete, or produce an empirical equation based on data collected in labs and/or actual construction.The vibration, according to Gardner and Quereshi (Gardner & Quereshi 1979), is done to fluidise the concrete, reducing its friction and shear strength.

Climbing formwork differs from traditional formwork in that it doesn't need to be repeatedly erected. Additionally, the addition of a scaffolding structure to provide support from the ground to the construction site is superfluous. The result is that building progress can be accelerated. During construction, the use of self-climbing formwork reduces labour costs, minimises crane downtime, and improves safety and convenience for workers at heights. After the formwork's use is over, it can be completely recovered, restored, and used again for projects with structural components that are exactly the same or quite similar (Jacquet et al. 2009).

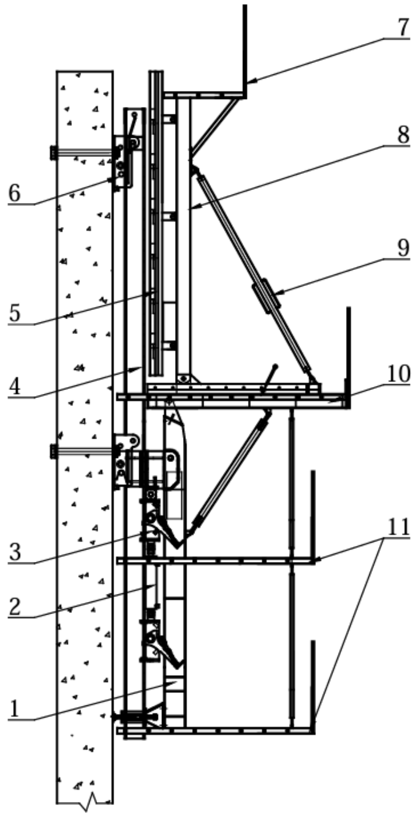

Figure 1: 1. Structural diagram of a self-climbing formwork. 1. Lifting frame, 2. Hydraulic system, 3. Rail climbing apparatus. 4. rail, 5. formwork shell,
6. climbing shoes, 7. Concreting platform, 8. mainframe, 9. cross brace, 10. main platform, 11. under platform

Various novel research studies can be used to general vertical formworks. This includes studies on the computation of fresh concrete pressure on the formwork shell surface (Graubner et al. 2012) (Puente et al. 2010) and the impact of shell surface materials on lateral pressure (Arslan et al. 2005). For the climbing operation (Waldschmitt & Pauley 2003), a wall climbing form hoist was mentioned as a tool that can scale the wall to raise or lower the formwork.To diminish self-weight while preserving rigidity and flatness of the shell surface, the anti and supporting structures of formwork systems can be achieved through the combination of steel staging forms or the use of aluminium alloy materials.

Current research on self-climbing formworks concentrates on two areas. The first aspect is exploitation research aimed at enhancing efficiency, safety, and appropriateness for particular projects, such as evaluating their effectiveness (Kannan & Santhi 2013), ensuring safety during operation (Liu et al. 2012), optimising their structure for use in bridge towers with a 30-degree slope (Li et al. 2014), and addressing the formwork vibration response induced by wind at elevated heights. The alternative involves research aimed at enhancing their attributes. In this second aspect, the scientific publications are predominantly disseminated by patent offices and concentrate on their two principal functions.
Climbing rail extension components were developed for uncomplicated ascents from the lower levels of concrete edifices (Schwoerer 2014) A rack-and-pinion gear could be utilised to move the formwork shell in order to open and close it. Apart from its ability to be opened and closed, the formwork can also be modified to build overhanging constructions. One of the solutions that is frequently used nowadays is this invention.

Recommended methodologies to improve the opening and closing of the shell

Throughout the course of numerous generations, the ascending formwork system has developed progressively more comprehensive features. The capacity to automate the construction process remains a persistent challenge for them. In order to enhance the efficiency of formwork, this article introduces alternative methods for two standard processes. These methods are based on the investigation and evaluation of the structural principles of contemporary climbing formwork types. These recommendations deal with the calculation and design of a climbing formwork that has a 4 m by 3 m shell.
The quality of concrete surfaces is also improved by the application of the solution, and the structure of the associated formwork ensures compactness and rigidity.

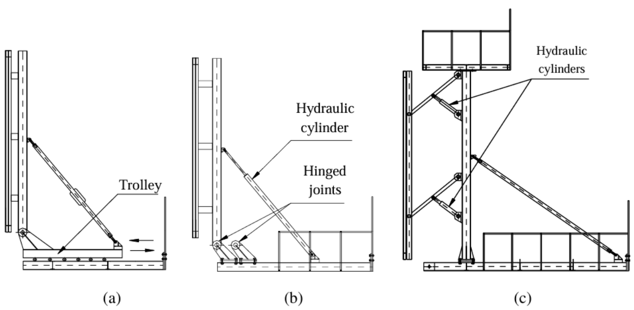

Figure 2 : three methods of closing and opening of shells (Nguyen et al. 2019).

Method (a) trolleys: There are numerous methods for opening and closing climbing formwork, each of which has its own trade-offs in terms of precision, cost, and simplicity. The formwork shell is mounted on trolleys or sliding shoes that are affixed to the primary frame in the most basic approach. The workers roll the trolleys inward until the shell seats against the concrete face, lock it in place, pour, and then roll the assembly outward to separate and ascend for casting. The trolley-mounted method is both uncomplicated and cost-effective. Its rack-and-pinion or screw drives and basic slides ensure that manufacturing costs are kept low, while the inward travel of the shell allows for easy adjustment of the concrete thickness. Nevertheless, the system is more prone to play or misalignment under load, and the process of achieving uniform alignment across multiple panels can be time-consuming due to the fact that the shell and frame rely wholly on roller fit and manual shimming for stability.

Method (b) hydraulic cylinders and articulated joints: A more advanced approach involves the use of hydraulic cylinders to move the shell in and out, while the lower extremities of the frame pivot on articulated joints. The shell can be positioned against the form face with high repeatability, as the extension is controlled by valves and pipelines. The process is significantly more automated through remote or PLC integration. Calibration is simpler than in trolley systems, and accurate coplanarity between adjacent containers is easily maintained. However, the initial fabrication costs are significantly increased by the necessity of additional cylinders, pumps, and valves. Additionally, the geometry of the single-acting cylinders frequently restricts the range of adjustable concrete thickness, necessitating the re-pinning of the frame to different articulations in order to adjust form sizes.

Method parallelogram-link method (c) : Effectively integrates the advantages of both approaches by affixing each shell module to the frame with four hinged limbs and four hydraulic cylinders that are arranged in a parallelogram. The shell remains precisely parallel to the frame at all times as the linkage forces pure in-out translation as the cylinders extend or retract. This results in a wider adjustment stroke for concrete thickness, uniform coplanarity across panels, and exceptional accuracy. The system achieves extraordinary stiffness, stability, and automation readiness by reusing existing hydraulic power packs and bolting the frame rigidly to the climbing platform with cross-braces. The parallelogram-link design offers distinct performance advantages for projects that require tight tolerances and efficient, repeatable operation, despite the fact that it is associated with a higher cost and complexity of fabrication due to the additional link arms and hinge hardware. Thus, the principal drawback remains.

Criterion	Trolley-Mounted	Single-Act. Hydraulics	Parallelogram-Link Hydraulics
Installation Cost	Low	High	Moderate–High
Operational Simplicity	Simple (manual)	Moderate (hydraulics)	Moderate (hydraulics + linkages)
Positioning Accuracy	Fair	Excellent	Excellent
Thickness Adjustability	Excellent	Limited	Excellent

Automation Potential	Low	High	High
Structural Rigidity	Moderate	High	Very High

An innovative rail locking mechanism

The hydraulic approach has become the dominant method for self-climbing formwork, as it eliminates the necessity for external cranes and enables construction to be conducted at an almost infinite height. This is why it is now ubiquitous in high-rise construction. Climbing formwork on a vertical plane can be accomplished using rope hoists, cranes, or hydraulic systems. By directly anchoring hydraulic jacks or cylinders to the previously cast wall, a conventional formwork is transformed into a self-climbing system. The anchors sustain the load as each lift is completed, and the formwork "climbs" itself to the next level.

In terms of hydraulics, there are two primary variants. The initial method illustrated in figure involves using both odd and even sets of hydraulic jacks, which are single-acting, to push the formwork higher by alternating locking to the wall anchors. The formwork is lifted and held by the even jacks in a single sequence, while the odd jacks retract, detach, re-anchor higher up, and then hold while the even jacks recalibrate. Each cycle, the entire frame is raised by the jack stroke by repeating this swap-and-lift sequence.

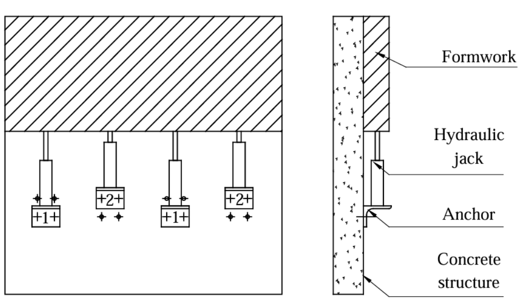

Figure 3: The principle controlling the lifting process of formworks through the utilisation of hydraulic jacks of a parity type (Nguyen et al. 2019).

In the second variant, a cylinder is mounted on movable rails with specialised one-way clamping devices, which combine lifting and anchoring. The cylinder extends to elevate the formwork during a frame-lifting cycle, during which all clamps engage, the top clamps release, and the cylinder retracts into position for the next lift. The top clamps re-engage, and the bottom clamps release, allowing the cylinder to retract. In the subsequent rail-lifting cycle, the bottom clamps remain in place, the top clamps are released, and the piston is driven downward to raise the rails (and their affixed anchors) along the same stroke. Subsequently, the clamps are exchanged, and the cylinder is reset.

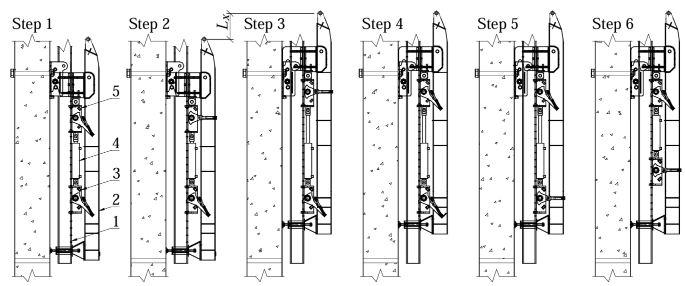

Figure 4: The elevating cycle of the lifting apparatus. 1. Rail, 2. Lifting frame, 3. Under-rail clamping device, 4. Hydraulic cylinder, 5. Upper-rail clamping device (Nguyen et al. 2019)

Reliable rail-clamping devices are necessary for the rail-and-cylinder system, which reduces the number of necessary cylinders by half, reduces the overall cycle time, and produces a compact, readily attached formwork package. Both hydraulic methods are the preferred choice for the construction of tall, repetitive concrete walls, as they significantly outperform crane- or rope-based climbing in terms of speed, safety, and mechanisation potential.

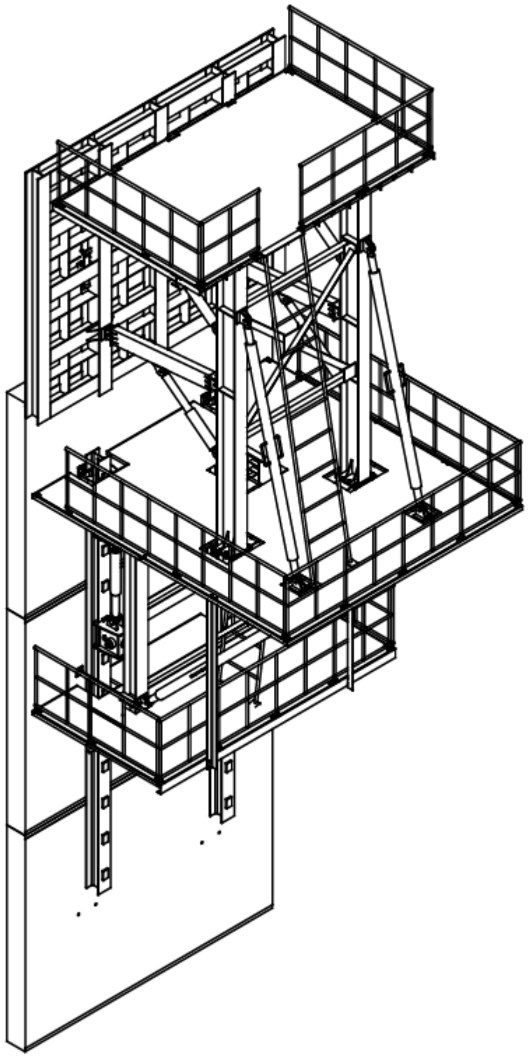

Figure 5: The hydraulicself-climbing formwork withthe shell's working (Ye et al. 2024)

Clamping device component

The clamping devices are cleverly constructed using a one-way gearbox for each device to reduce the amount of hand movement required to open and close them. Operators will then determine each clamping device's functioning orientation. Each device in a formwork lifting operation has a two-turn directional setup period.

1. Spring-Loaded One-Way Anchors

These simplest devices rely on a pre-compressed spring that pushes an anchor pawl into engagement with a fixed rail lug or tooth. In its resting state the spring holds the anchor firmly against the rail (Waldschmitt & Pauley 2003), so that even if hydraulic pressure is lost the formwork remains positively supported. When it's time to reposition, a small hydraulic or manual actuator rotates a cam or "shake bar" to compress the spring further and swing the anchor clear of the lug. Because the mechanism is entirely mechanical once set, clamp-housing size can be kept small and no continuous power is required to maintain holding force. Their downside is that release and re-anchoring sequences are relatively slow and often require exact timing of multiple devices in concert.

2. Cam-Actuated Clamps

Cam-type devices use a rotary actuator—or in simpler systems, a lever—that turns a cam profile against the rail or a bearing surface. As the cam rotates, its eccentric shape either presses a hardened pad into the rail to lock or retracts it for release. These clamps can be extremely compact and provide very high clamping forces with modest actuator torque. Cams also allow taper-shaped grips that self-adjust to minor rail misalignments. However, because the grip relies on friction, maintenance of clean cam surfaces and sufficient preload is critical for safety, and the mechanism can be sensitive to debris or concrete splatter.

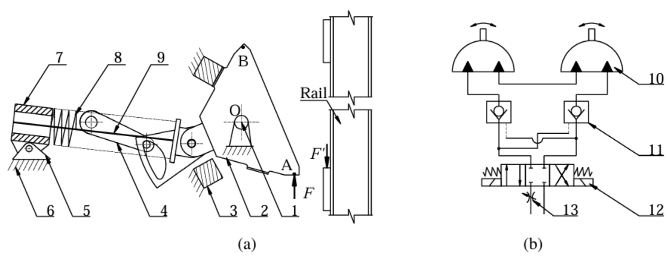

Figure 6: Claming device: two components: a) the device's construction schematic; and b) a hydraulic circuit for managing rotary actuators. 1. A horizontal shaft 2. shakebar, 3. carrier, and 4. anchor 5. Clamphousing, 6. lid, 7. a hydraulic rotary actuator, 8. a shaft button, and 10. a spring 9. Shaft that is inclined11. Pilot-operated check valve, 12. Directional

valve, and 13. Variable throttle valve (Nguyen et al. 2019)

3. Hydraulic-Cylinder Directional Clamps

Building on the spring-anchor concept, the hydraulic-cylinder variants incorporate a small cylinder (or rotary actuator with piston) to actively swing the anchor through a controlled angle. In the device you describe, a hydraulic cylinder drives a shake bar which, via an articulated joint, shifts the spring-loaded anchor between two support orientations (points A and B). Precise positioning is held by pilot-operated check valves (de la Manutention 1998), while variable-throttle valves control actuation speed for smooth engagement. These clamps combine positive mechanical locking with remote, programmable control—ideal for fully automated climbs—yet add the complexity of hoses, valves and pilot lines.

4. Rail-Clamp Assemblies with Integrated Slides

Some systems integrate the clamp into a sliding carriage (En 2003)that runs up and down special rails. Here, clamping elements are housed within a carriage that uses hydraulic pistons both to lift the carriage and to engage its clamp jaws. One-way check valves ensure that once the carriage is clamped it cannot drift downward, and dedicated cylinders handle rail-pulling and frame-lifting in interleaved cycles. By consolidating lifting and locking into the same unit, these assemblies reduce part count (sometimes halving the number of cylinders) and shorten cycle times—but they depend on robust, precisely machined rails and reliable clamp jaws to avoid binding.

Stress and displacement of element

Using the article's (de la Manutention 1998) recommendations, a self-climbing formwork with a 4 m by 3 m working shell size was created. It is confirmed by the test findings that the requirements meet the standard. Stress is present in the two main parts of the rail clamping device, and the maximum stress values that can be found in these parts under the most severe conditions are lower than the allowed stresses of structural steel used to make formwork. They also have low maximum displacement values. These metrics demonstrate the safety and security of their job.

The horizontal displacement perpendicular to the concrete surface of the shell is fairly substantial due to the most unfavourable loading conditions during the concrete pouring process. This limitation is overcome by adjusting the primary displacement forward (towards the concrete structure) by 0.2 degrees in the first erection when they support the maximum load. The displacement of the shell surface after the concrete pouring process is examined using three vertical and three horizontal lines.

(1) $1.1(G + G_h + q_f + q_w + q_v + q_b + q_c)$,

(2) $1.1(G + G_h + q_f + 3q_w + q_v + q_b + q_c)$, since

$G = gravity\ of\ structure$,

$G_h = gravity\ of\ the\ hydraulic\ system$,

$q_f = load\ combination\ by\ equipment,\ materials\ and\ workers$

, $q_w = wind\ load$,$q_v = concrete\ vibrator\ load$,

$q_b = concrete\ pouring\ pressure\ load$,

$q_c = horizontal\ pressure\ of\ cement\ concrete$

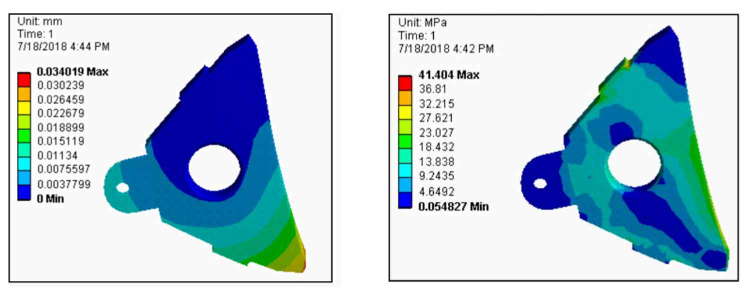

Figure 7: stress and strain of the nachor

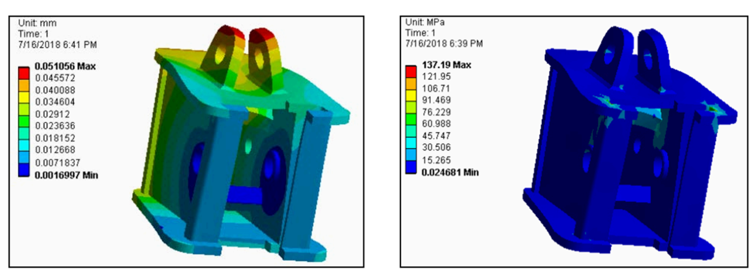

Figure 8: stress and displacement of th ehousing of the anchor

The outcome aligns with the structure's deformation concept. There are concave and convex zones on the concrete surface that the climbing formwork sculpted. When formworks are used to form the concrete structure's surface during the pouring process, such phenomenon is unavoidable (2013-04 2013).

Lateral pressure of concrete pouring

Theoretical Model:

Forming and working platforms that may climb themselves are the subject of direct analysis. When it comes to these ideas, the most significant problem is that the value of "λC" does not remain constant. It can range from one when concrete operates as a fluid to zero when concrete is capable of self-sufficiency.

These theories' two instances (Schjødt 1955). While (Levitsky 1973) theory is used in the later, soil mechanics ideas are used in the former, ignoring concrete cohesiveness. A great deal of complexity in the models used to design formwork is unnecessary because of the many variables related to the properties of the concrete, the formwork, and the placement technique that affect the lateral pressure, friction on the wall, and deformation. (3) $P = \lambda_c \gamma H$,

$\lambda_c = vertical\ and\ horizontal\ pressure\ relationship$,

$\gamma = specific\ weight\ of\ concrete, H = depth$

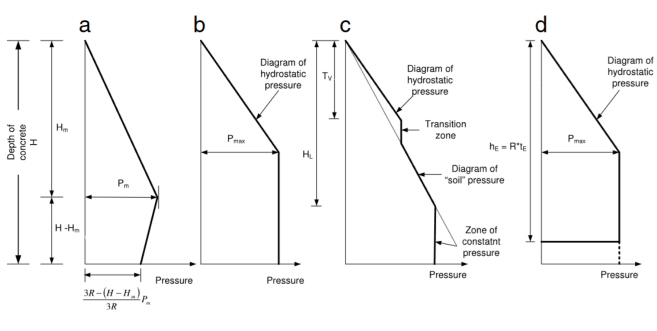

Figure 9: Pressure digram of different experiments

The pressure is currently predicted using empirical approaches, and when these methods are extrapolated outside of the area where experimental data is available, certain issues occur.

According to reports (The Concrete Society 1997) , the experimental models were categorised as either those that were applied to walls and bases or those that were used in columns. parts where either the width or the breadth exceed two meters are referred to as walls or bases, whereas parts of a column have both dimensions less than two meters.

This investigation is necessary due to the absence of experimental data for concrete chunks with cross-section diameters beyond 2 m.

The pressure at any particular point within the form varies over time, as stated by (Hurd 2007). The designer typically does not require a detailed understanding of the variation. The utmost pressure envelope that can be applied to the form is the significant magnitude.

The experimental models attempt to determine the pressure envelope by utilising the minimum parameters that can be utilised in the design process. Experimental distributions of base and wall pressures are illustrated below: Consideration of the fluid properties of fresh concrete was the most conventional and conservative approach. In this manner, it is necessary to consider the hydrostatic pressure distribution on the form walls illustrated in figure 9 a . (3) $H_m = 1.63R^{1/3}$,(4) $P_{max} = 23.4H_m$,

$H_m = head\ of\ maximum\ lateral\ pressure$,

$P_{max} = lateral\ pressure\ agaisnt\ formwork\ (kPa)$,

$R = rate\ of\ placement\ (m/h)$

The author (Adam et al. 1965) recommends the use of correction curves during the development of equations for a specific combination, temperature, density, and decline, where the parameters are distinct.

A laboratory experiment was conducted on a formwork that was 3 meters in height, 2.5 meters in breadth, and had a thickness of 8 to 30 centimetres in a study. The team's goal was to ascertain the influence of vibration, sag, cement type, rate of placement, and aggregate size on the lateral pressure. The rate of placement, the type of cement, and the size of the aggregate were identified as the most critical variables.

The pressure distribution proposed by these authors is depicted in Figure 9 b, with the value of P_{max} denoted by Equation 5. The hydrostatic pressure generated by a liquid with a density of 2400 kg/m3 is never greater than 23.54H.

$5(a)\ P_{max} = 19.62 + 12.26R,\ T \leq 5^{\circ}C,$

$5(b)\ P_{max} = 19.62 + 12.81R\ ,\ T = 5^{\circ}C,$

$5(c)\ P_{max} = 19.62 + 8.34R,\ T \geq 25^{\circ}C,$ When $R > 2m/h$,

$5(d)\ P_{max} = 4.22 + 1.96R,\ T \leq 5^{\circ}C,$

$5(e)\ P_{max} = 35.32 + 1.96R,\ T = 5^{\circ}C,$

$5(f)\ P_{max} = 32.37 + 1.96R,\ T \geq 5^{\circ}C$ since

$P_{max} = lateral\ pressure\ (kPa),$

$R = rate\ of\ placement\ (m/h),$ $H = concrete\ depth,$

$T = concrete\ temperature$ and

$(6)\ P_{max} = 24h_i + \frac{3000HP}{d} + \frac{d}{40} + \frac{400R^{1/2}}{18+T} \times (\frac{100}{100-\%F}) + \frac{\alpha-75}{10}$ after conducting numerous experimental studies (Gardner 1982), a pressure envelope was proposed in accordance with Figure 9 b, with the value of pressure determined by Eq. (6).

The hydrostatic pressure generated by a fluid with a density comparable to that of concrete is the utmost pressure that can be achieved. He determined that the maximal lateral pressure was contingent upon the concrete temperature, sag, rate of placement, depth of vibration, and percentage of fly ash or slag in the mix.

$HP = vibrator\ power,\ \ \%F = fly\ ash\ or\ slag\ precentage,$

$\alpha = concrete\ slump\ (mm),$

$d = minimum\ form\ dimension\ (mm)$. The initial zone, which is subject to hydrostatic pressure up to a variable height T_v, is contingent upon the profundity of each lift and the vibratory methods discussed by (Palanca 1982). For the last lift, he suggests setting T_v to a maximum of 1.0 m.

Before reaching the granular zone, there is a transition zone that maintains a consistent pressure during the whole process. Hydrostatic pressure is influenced by a coefficient of active pressure K_a in this region, which is a relationship between vertical and horizontal pressure. This coefficient is contingent upon the inclination of the form wall and the internal friction between particles.

$(7)\ K_a = \frac{sin^2(\frac{\pi}{4}-\frac{\varphi-\varepsilon}{2})}{cos^2(\frac{\pi}{4}-\frac{\varphi+\varepsilon}{2})}$

$\varphi = internal\ friction\ of\ concrete\ angle,$

$\varepsilon = iclination\ of\ the\ form\ wall,\ \ (8)\ tg\varphi = \frac{260-\alpha}{1400}$ since

$\alpha = concrete\ slump\ (mm)$

The distribution is sustained until the formwork is completed, or until the pressure limits H_L are reached. This distribution is sustained until the formwork is completed, or until the pressure limits are reached, as illustrated in Figure c. $(9)\ H_L = T_V + Rt_0,$

$H_L = transition\ depth\ between\ thrid\ and\ fourth\ zone,$

$T_v = transition\ deoth\ betwen\ first\ and\ second\ zone\ (m)$,

$R = rate\ of\ placement\ (m/h),$

$t_0 = setting\ time\ of\ concrete\ (h)$ (Graubner et al. 2012) and $(10)\ t_0 = \frac{70+0.3\alpha-2T}{25+T}$,

$(11)\ P_{max} = [C_1\sqrt{R} + C_2k_1\sqrt{H_1 - C_1\sqrt{R}}]\gamma$

$C_1 = 1\ depending\ on\ the\ size\ and\ shape\ of\ formwork,$

$C_2 = coefficient\ that\ depends\ on\ the\ constituent\ materials\ of\ conc$

$\gamma = concrete\ specific\ wieght\ (kN/m^3)$,

$H_1 = vertical\ from\ height\ (m)$,

$R = rat\ of\ placement\ (m/h)\ (12)\ K_1 = (\frac{36}{T+16})^2$

according ot the figure b the volume of the maxiumum lateral pressure P_{max} can be determined based on the following

$(13)\ P_{max} = C_mC_f[31.1 + 7.8H - 0.5(T + 17.8 + 0.8(\alpha)^{1/2} - 14.8log(t)],$

$C_m = constituent\ materials\ of\ concrete\ coefficient,$

$C_f = 1.2\ for\ columns$, (14 a) $P_{max} = C_W C_c[7.2 + \frac{785R}{T+17.8}]$, $R < 2.1m/h$ and $H > 4.2\ m$ and $2.1m/h < R < 4.5m/h$, (14b) $P_{max} = C_w C_c[7.2 + \frac{1156}{T+17.8} + \frac{244R}{T+17.8}]$ since $P_{max} > 30C_W$ $C_w = unit\ weigh\ coefficient$, $C_c = chemistry\ coefficient$

Climbing Platform

The direct analysis method was introduced by the Standard for the Design of Steel Structures GB50017-2017, which was implemented in China in 2018 (of Housing and Urban-Rural 2017) . The direct analysis method incorporates the initial defects of the overall structure and components, contemplating "P-Δ-δ," in contrast to the first-order linear design method based on the calculation length coefficient method. For component stability analysis, the calculated length coefficient method is not necessary. This is because nonlinear analysis and load-bearing capacity verification of second-order structural effects are not necessary. Nevertheless, this technique is unable to directly build various load combinations after they have been calculated separately, as it is a non-linear analysis. Before conducting an analysis, it is imperative to combine the stresses and apply them to the structure.

Nida software was utilised to analyse steel frame structures in order to investigate the application and research of the direct analysis method in a variety of structures. They discovered that the direct analysis method is more precise and efficient than the first-order design method, which is based on the computational length coefficient method (Ye et al. 2024). The effectiveness and reliability of the direct analysis method for structural analysis of semi-rigid connected steel structures were confirmed by Shu Ganping et al. through a comparison of the calculation results with experiments (Ganping et al. 2014).

A direct analysis and optimisation method for semi-rigid structures was further developed by (Shu et al. 2014) . Furthermore, Ding Zhixia et al. conducted a study on the continuous collapse of structures using the direct analysis method and compared it to conventional design methods (Ye et al. 2024). The stabilising capacity of spanning plane trusses was examined by Zhao Lei et al in an investigation of the impact of initial geometric defects (Lei et al. 2022). There has been no application of direct analytic methods to the structural design of building formwork, despite the fact that it is commonly used in existing research as a typical steel frame structure optimisation of cable structures (Zheng et al. 2019). Various structures have been effectively analysed using the direct analysis method in previous research (Hong & Jung 2022).

Structure Diagram

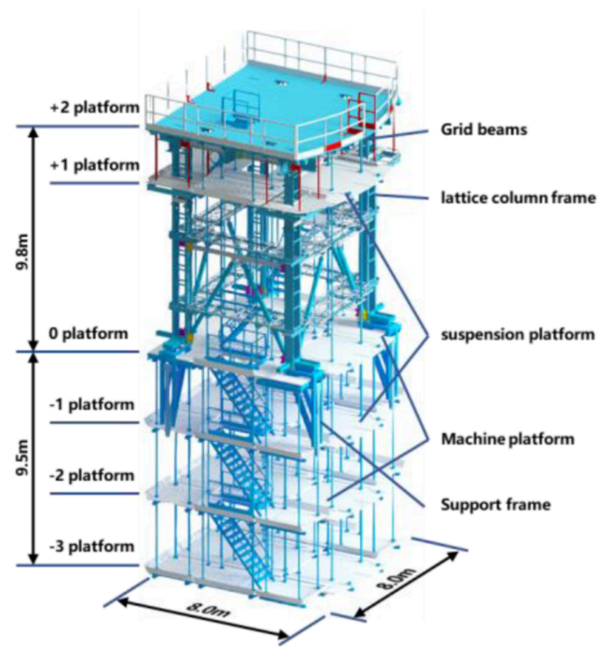

Figure 10: Structures of an SCP (Ye et al. 2024).

Figure above illustrates the SCP utilised in the construction of the core tube of a high-rise building. This system comprises machine platforms, suspension platforms, the grid beam, the lattice column frame, and support frames. The research of structure structure conducted by (Ye et al. 2024) comprises six longitudinally orientated operation platforms, with a positive platform height of 9.8m and a negative platform height of 9.5m. The total height of the structure is 19.3m, and its horizontal dimension is 8m×8m.

The principal function of the negative platform is to serve as the maintenance platform. The 0-level platform is the operation platform for formwork, while the +1 and +2 platforms are utilised for the piling of loads, reinforcement binding, and concreting. The SCP structure's force transfer is evident. Two components comprise its force transmission path, as illustrated in Figure 2. One method involves the transmission of the load from each suspension platform to the secondary beam of the +2 platform via the suspension rods. The load is subsequently transferred to the support frame via the grid beam and the lattice column. Another method involves the direct transmission of the load from each negative machine platform to the 0-level machine platform via the suspension rod. The zero-up machine platform is directly connected to the lattice column to transmit the load to the support the load of the frame of a downward force.

In order to convey the loads to the core-tube, the support structure is anchored to the core-tube by pre-embedded anchors (dowels).

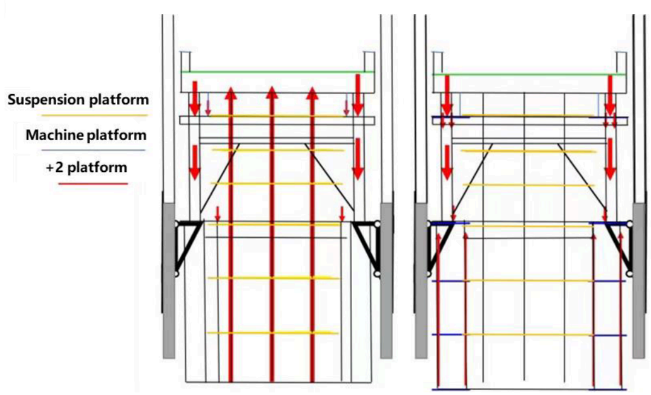

Figure 11: Direction of the force transmission path.

Analysis of the self climbing formwork platform

The SCP's suspension platform stiffness is exceedingly low due to its structural characteristics, and its buckling mode is evidenced by the lateral deformation of each suspension platform. The evaluation of the overall initial defect of the structure in accordance with the first-order buckling mode is inconsistent with the objective of the structural initial defects that were implemented. In accordance with the Standard for the design of steel structures, the initial geometric defects representative value Δni at the corresponding story height can be supplemented by the overall initial defects if the structure has a regular shape and significant story separation.

(15) $\Delta_{ni} = \frac{h_i}{250}\sqrt{0.2 + \frac{1}{n_s}}$,

$\Delta_{ni} = total\ gravity\ load\ design\ value\ for\ the\ i^{th}\ floor$,

$n_s = total\ number\ of\ layers\ in\ the\ sructure$,

$h_i = height\ of\ calculated\ floors$ (16) $\delta_0 = e_0 sin\frac{\pi x}{l}$,

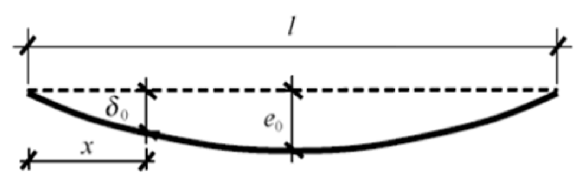

Figure 12: deflection of a member

Nonlinear analysis and verification

After the structure is subjected to various combinations of stresses, the nonlinear analysis is conducted. The internal forces in the members, which were obtained from the analysis, are substituted into Eq. (17) for verification.

$\frac{N}{A_f} + \frac{M_x^{ii}}{M_{cx}} + \frac{M_y^{ii}}{M_{cy}} \leq 1.0$ $N = design\ value\ of\ axial\ force$,

$A = gross\ section\ area$,

$f = design\ value\ of\ stregth\ of\ steel$,

$M_x^{ii}, M_y^{ii} = design\ bending\ momemnt\ x, y\ axis\ respectively$

The primary and secondary beams are simplified from stacked to intersecting, and a wireframe model is created using 3D drawing software in accordance with the centerline of the members. However, the stresses are only applied to the secondary beams. With respect to the actual connections, the nodes are simplified as either inflexible or hinged. Figure above illustrates the hinged supports that constitute the structure's boundary conditions. Q235B is the steel that was utilised in the model. The dead loads in addition to the structure's self weight encompass those burdens that are permanent, including pavements, handrails, stairs, formwork, and ancillary structures. The live loads are the working conditions of the SCP, as determined by the working condition load planning. Table 1 displays the live load cases. The fundamental combination of "1.3×DL+1.5×LL" is employed for the bearing capacity and bearing reaction in the load combinations, while the conventional combination of "1.0×DL+1.0×LL" is employed for the displacement calculation. The standards are used to determine these combinations.

Support reactions

The vertical support reaction force of each support is extracted according to the basic combination of loads, as illustrated in Table 2. The SCP in the example has four supports (Fig. 6), which are fixed to the core-tube. Their design is a critical factor in ensuring the structural reliability and construction safety.

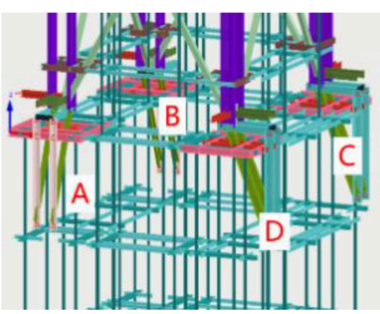

Figure 13: support fixed points

ID	First order linear analysis/kN	Direct analysis/kN	δ/%
A1	15.65	19.63	25.43
A2	25.44	25.51	0.28
A3	173.02	170.87	-1.24
A4	179.78	177.52	-1.26
B1	22.84	23	0.7
B2	16.89	20.69	22.5
B3	179.56	177.3	-1.26
B4	174.24	172.05	-1.26
C1	30.35	29.78	-1.88
C2	12.2	13.98	14.59
C3	184.41	183.57	-0.46
C4	176.44	176.56	0.07
D1	13.21	15.25	15.44
D2	28.25	27.73	15.44
D3	178.76	178.66	-0.06
D4	184.7	183.63	-0.53
Total	1595.74	1595.74	0.0

Table 1: support reaction forces

The maximum support reaction force of both the first-order linear analysis and the direct analysis was 184.7kN and 183.6kN, respectively, in the D4 support. The relative error between the two was a mere 0.58%. The total support reaction forces were nearly identical as a result of the identical applied loads.

The maximum relative error was observed in support A1, which reached 25%. However, the absolute error was only 3.98kN, which is still negligible in comparison to the structure as a whole. This is indicative of the feedback to the support reaction force's performance. It is evident that the direct analysis method can provide the design parameters for a reasonable support in this project, as well as the total support reaction force. After taking into account the initial defects of the support frame members, this is the performance of the direct analysis method.

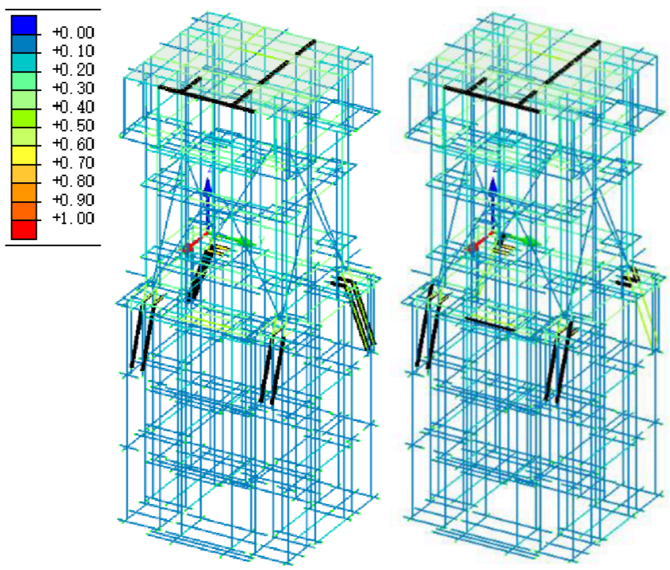

Figure 14: Stress ratio

Figure 15: Main frame structures

The maximum stress ratio for first-order linear analysis was 0.801, while the maximum stress ratio for the direct analysis method was 0.799. The secondary beams of +2 beams, the secondary beams of 0 platform, and the diagonal supports of the support frames were the elements with a stress ratio greater than 0.5 in both methodologies, as illustrated in Fig. 7.

The design results of the direct analysis method and first-order linear analysis in NIDA were compared. The average stress ratio difference was 0.0014 after the two were compared. In general, the results of the two were relatively similar, with 91.1% of the unit stress ratios varying between -0.01 and 0.01. A total of 119 elements with stress ratios exceeding 0.01 were designed using the direct analysis method, and statistics were conducted on elements with stress ratios exceeding 0.01.

A total of 119 elements were identified as having higher stress ratios using the direct analysis method, and statistics were conducted on units with stress ratios exceeding 0.01. The majority of them, 64.7%, were horizontal members, primarily bending members. A total of 52 elements with a comparatively low stress ratio were analysed using the direct analysis method. Of these, 73.1% were non-horizontal members, primarily axial and compression bending members. This is due to the fact that the SCP structure is a typical vertical structural system, and the stress ratio increases as the initial defect design bending moment increases, resulting in an increase in the horizontal bending members. The principal compression members are the vertically distributed members, and the first-order linear analysis is more unfavourable than the actual situation due to the direct consideration of the calculated length factor.

Componen t	Before	After	Weight loss
Machine platform beams	C 20B	C 20B	-

0.5 story platform beams	C 16B	C 16B	-
Platform primary beam	C 10	2C 100×50×4	40.19
Suspension rods	F 50×5	F 50×4	51.59
Grid beams	HM 594×302×14/23	HN 600×200×10/15	37.33
+2 stoey secondary beam	2C 10	2C 14B	45.76
Lattice column	C 40B	C 40A	-67.85
Support frame beam	C 14B	C 14B	9.60
Support frame column	L 200×125×16	L 200×125×16	-
Support frame diagonal	C 22B	C 22B	-
Main frame diagonal supports	J 160×130×8.5/9.6	J 160×130×6/6	-

Table 2: structural cross section optimization

There is a lot of room for optimisation in this case because the SCP structure has a big self-weight and most of its members are under mild stress. To achieve high efficiency and light weight, the optimisation focused on cross-section optimisation, maintaining the original node connection mode and minimising excess cross-sections for assembly convenience. The safety margin of the support anchorage point can be enhanced, and the support reaction force can be further reduced by reducing the self-weight of the structure.

The cross sections of certain members were optimised, and Table 2 illustrates the comparison of the cross sections before and after optimisation. After optimisation, the total weight decreased from 35.02 tonnes to 26.05 tonnes, a reduction of approximately 25.63%.

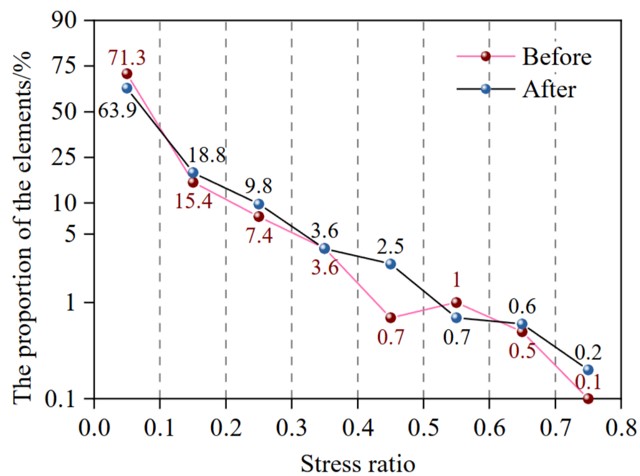

Figure 15: distribution of the percentage elements with respect to stress ratio

The overall distribution pattern analised by (Ye et al. 2024) remained consistent with that in place prior to optimisation. The elements with stress ratios exceeding 0.5 were converted to 0-story and +1-story platform beams, which were not incorporated into the main frame elements. In comparison to the pre-optimization, the stress ratios of the main frame diagonal supports, the machine platform, and the +2 platform elements have been decreased. In Figure 15, the distribution of the stress ratio-number of elements before and after optimisation is illustrated. The number of high stress ratio elements did not increase significantly after the 25.63% reduction in steel usage. Further, the percentage of elements with stress ratios greater than 0.4 increased by only 4% from 2.3%, preserving a substantial safety margin. After optimisation, the number of elements with stress ratios less than 0.1 was reduced as a result of the large number of horizontal elements.

Conclusion

The capacity of self-climbing formworks to automatically mate the building process is a constant issue. The group proposed solutions for two regular operations in order to enhance the automatic level of ascending form works. They consist of the opening and closure of the formwork shell and the ascending operation.

(1) The direct analysis method is more efficient and straightforward than the first-order linear design method, which is based on the computation of length coefficients, for the design and optimisation of SCP.
(2) The results of the direct analysis are essentially consistent with those of first-order linear analysis. The primary cause of the discrepancy is the divergence in calculation methodologies between the two.
(3) The direct analysis method was employed in the above example to achieve a 25.63% reduction in steel consumption through cross-sectional optimisation, all while maintaining a high safety margin. Detailed construction of structural connection elements is not completely considered by the direct analysis method. Subsequently, it is intended to implement node performance analysis in the future to ascertain the semi-rigid parameters of each node. This will enable the development of multi-scale optimisation designs.
(4) The proposals demonstrated exceptional benefits, including the reduction of execution time, the enhancement of the quality of the casted concrete surface, the safety of operation, the reduction of labour, and the maximum mechanisation of the formwork's working processes.
(5)The uniformity of the concrete surface following casting is directly influenced by the rigidity of the formwork structure.
(6)The closure or opening of various formwork shells, as well as the ascending procedure of multiple formworks, can be done concurrently.
These solutions can be implemented to either enhance the existing ascending formwork or create a new one, how ever the self-climbing formwork can be used to make the application either individually or simultaneously.

References

2013-04, D. 18202:, 2013. Toleranzen im Hochbau--Bauwerke.

Adam, M., Bennasr, M. & Santos, D.H., 1965. Poussée du béton frais sur les coffrages. Ann Inst. Technique Bâtiment Travaux Publics, Paris, 78, pp.403–423.

Arslan, M., Şimşek, O. & Subaşı, S., 2005. Effects of formwork surface materials on concrete lateral pressure. Construction and building materials, 19(4), pp.319–325.

En, B.S., 2003. 12811-1: 2003, Temporary works equipment--Part 1: Scaffolds--Performance requirements and general design. British Standards Institution, London, UK.

Ganping, S., Wei, L. & Siulai, C., 2014. Theoretical research on direct analysis method for semi-rigid steel frames. Journal of Building structure.

Gardner, N.J., 1985. Pressure of concrete on formwork-A review. Journal Proceedings, 82, pp.744–753.

Gardner, N.J., 1982. The effect of superplasticizer and flyash on formwork pressures. Forming Economical Concrete Buildings, Portland Cement Association.

Gardner, N.J. & Poon, S.M., 1976. Time and temperature effects on tensile, bond, and compressive strengths. Journal Proceedings, 73, pp.405–409.

Gardner, N.J. & Quereshi, A.R., 1979. Internal vibration and the lateral pressure exerted by fresh concrete. Canadian journal of civil engineering, 6(4), pp.592–600.

Graubner, C.-A. et al., 2012. Formwork pressure induced by highly flowable concretes – design approach and transfer into practice. Structural concrete, 13(1), pp.51–60.

Hong, G.-H. & Jung, S.-W., 2022. Development of auto-climbing formwork system for composite core walls. Journal of Asian architecture and building engineering, 21(2), pp.511–520.

of Housing and Urban-Rural, M., 2017. GB 50017-2017: Standard for Design of Steel Structures.

Hurd, M., 2007. Lateral Pressures for Formwork Design. Concrete international, 29, pp.31–33.

Jacquet, P. et al., 2009. Formwork and falsework for heavy *construction. Available at: https://research.tudelft.nl/en/publications/formwork-and-falsework-for-heavy-construction.*

Kannan, M.R. & Santhi, M.H., 2013. Constructability assessment of climbing formwork systems using building information modeling. Procedia engineering, 64, pp.1129–1138.

Kopczynski, C., 2008. Formwork efficiencies. Concrete international, 30, pp.41–43.

Lei, Z. et al., 2022. Influence of Initial Geometric Imperfection on the Stability Bearing Capacity of a Cross-Story Plane Truss". Progress in Steel Building Structures, 24(04), pp.66–73.

Levitsky, M., 1973. Analytical determination of pressure on formwork. Journal of the Engineering Mechanics Division, 99(3), pp.551–564.

Li, J.P. et al., 2014. Simulation analysis and structure optimization of steel structure climbing formwork with material properties used in the large angle leaning bridge tower. Applied Mechanics and Materials, 540, pp.201–204.

Liu, X. et al., 2012. Safety control of hydraulic self-climbing formwork in south tower construction of taizhou bridge. Procedia engineering, 45, pp.248–252.

de la Manutention, F.E., 1998. FEM 1.001; Rules for the design of hoisting appliances.

Mohan Sai, G. & Aravindan, A., 2020. A comparative study on newly emerging type of formwork systems with conventional type of form work systems. Materials today: proceedings, 33, pp.736–740.

Nguyen, V.T., Nguyen, K.A. & Nguyen, V.L., 2019. An improvement of a hydraulic self-climbing formwork. Archive of Mechanical Engineering, 66(4), pp.495–507.

Palanca, M.J., 1982. Presión del hormigón fresco. Monografía.

Peurifoy, L.R. & Oberlender, D.G., 2011. Formwork for Concrete Structures 4th edition. Available at: https://thuvienso.dau.edu.vn:88/handle/DHKTDN/8265.

Puente, I., Santilli, A. & Lopez, A., 2010. Lateral pressure over formwork on large dimension concrete blocks. Engineering structures, 32(1), pp.195–206.

Schjødt, R., 1955. Calculation of pressure of concrete on forms. Proceedings of the American Society of Civil Engineers.

Schwoerer, A., 2014. U.S. Patent No. 8,673,189. US Patent 8,673,189. Available at: https://patentimages.storage.googleapis.com/07/fd/7c/10a38c9d3e58d4/US8673189.pdf.

Shu, G., Wei, L. & Siulai, C., 2014. Theoretical research on direct analysis method for semi-rigid steel frames". Journal of Building structure, 35(08), pp.142–150.

The Concrete Society, 1997. Formwork: A guide to good practice, London, England: Thomas Telford.

Waldschmitt, T.J. & Pauley, R., 2003. U.S. Patent No. 6,557,817. US Patent 6,557,817. Available at: https://patentimages.storage.googleapis.com/1c/57/bb/217d200c5a998f/US6557817.pdf.

Ye, G.H. et al., 2024. Direct analysis method in self-climbing forming and working platform. ADVANCED STEEL CONSTRUCTION, 20(2), pp.144–148.

Zheng, Y., Suduo, X. & Lijun, W., 2019. Application of direct analysis design method in cable structure design". Construction Technology, 48(20), pp.1–4.